Validation of a virtual source model for Monte Carlo dose calculations of a flattening filter free linac

Jason Cashmore[a)]
Hall-Edwards Radiotherapy Research Group, University Hospital Birmingham NHS Foundation Trust, United Kingdom, B15 2TH

Sergey Golubev and Jose Luis Dumont
Elekta CMS Software, St. Louis, Missouri 63043

Marcin Sikora
Department of Oncology and Medical Physics, Haukeland University Hospital, Bergen 5021, Norway

Markus Alber
Section for Biomedical Physics, University Hospital for Radiation Oncology, Hoppe-Seyler-Str 3, 72076, Tübingen, Germany

Mark Ramtohul
Hall-Edwards Radiotherapy Research Group, University Hospital Birmingham NHS Foundation Trust, United Kingdom, B15 2TH

(Received 17 August 2011; revised 9 March 2012; accepted for publication 10 April 2012; published 22 May 2012)

Purpose: A linac delivering intensity-modulated radiotherapy (IMRT) can benefit from a flattening filter free (FFF) design which offers higher dose rates and reduced accelerator head scatter than for conventional (flattened) delivery. This reduction in scatter simplifies beam modeling, and combining a Monte Carlo dose engine with a FFF accelerator could potentially increase dose calculation accuracy. The objective of this work was to model a FFF machine using an adapted version of a previously published virtual source model (VSM) for Monte Carlo calculations and to verify its accuracy.
Methods: An Elekta Synergy linear accelerator operating at 6 MV has been modified to enable irradiation both with and without the flattening filter (FF). The VSM has been incorporated into a commercially available treatment planning system (Monaco^{TM} v 3.1) as VSM 1.6. Dosimetric data were measured to commission the treatment planning system (TPS) and the VSM adapted to account for the lack of angular differential absorption and general beam hardening. The model was then tested using standard water phantom measurements and also by creating IMRT plans for a range of clinical cases.
Results: The results show that the VSM implementation handles the FFF beams very well, with an uncertainty between measurement and calculation of $<1\%$ which is comparable to conventional flattened beams. All IMRT beams passed standard quality assurance tests with $>95\%$ of all points passing gamma analysis ($\gamma < 1$) using a 3%/3 mm tolerance.
Conclusions: The virtual source model for flattened beams was successfully adapted to a flattening filter free beam production. Water phantom and patient specific QA measurements show excellent results, and comparisons of IMRT plans generated in conventional and FFF mode are underway to assess dosimetric uncertainties and possible improvements in dose calculation and delivery. [http://dx.doi.org/10.1118/1.4709601]

Key words: Monte Carlo, flattening filter free, unflattened, virtual source model

I. INTRODUCTION

Therapeutic photon beams are generated by stopping a narrow electron beam in a metal target. These bremsstrahlung x-rays have a relatively constant angular energy spectrum, but a strongly forward peaked energy fluence which becomes more peaked as the initial electron energy increases. This translates into a triangular shaped beam profile.

To provide a more uniform fluence distribution, it is customary to insert a conical flattening filter (FF) of a high-Z material into the beam. The primary function of the filter is to provide a "nominally" flat radiation beam (e.g., at 10 cm depth), but in doing this, the filter causes negative side-effects such as

- changes in the spectrum due to differential photon absorption
- the need for the introduction of "horns" in the particle fluence to compensate for this angular variation of the spectrum
- a reduction in dose rate
- the creation of a significant source of extrafocal scattered radiation.

Such uniform beams can be advantageous for conventional treatments, but in practice, although a beam can be within flatness specification under uniform conditions (e.g., 10 cm depth in a homogeneous phantom with a flat surface), it may be significantly skewed taking into account realistic treatment geometries with inhomogeneities, body surface curvature, and treatment at depths other than the reference depth. Flattening filters have been regarded as an integral part of linear accelerators since their first medical use in the 1950s, but for beams with modulated intensity, an initially "flat" radiation distribution should not be necessary, and removing the filter will remove these disadvantages.

Several studies have reported flattening filter free (FFF) characteristics for Elekta,[1–3] and Varian[4–6] accelerators via direct measurement, Monte Carlo (MC) simulation, and by multisource modeling.[7] These studies demonstrate that filter free operation results in reduced leakage, higher dose rates, and simplified beam modeling. Further studies have also demonstrated that these properties result in significant reductions in doses to organs outside of the treated volume for equivalent delivery of intensity-modulated radiotherapy (IMRT) and SBRT plans on a prototype FFF Elekta linac.[8,9]

In theory, FF removal could increase the dosimetric confidence in a plan due to reductions in off-axis beam softening and by virtue of having less scattered photons and contamination electrons in the beam. The accuracy of the beam model could therefore be improved since we are reducing the uncertainty in these components. Coupling this with a Monte Carlo dose calculation algorithm could eventually lead to more accurate dose prediction compared to standard techniques.

The objective of this work was to model a FFF machine using an adapted version of a previously published virtual source model (VSM)[10–12] for Monte Carlo calculations and to test this implementation against standard phantom measurements and for delivery of clinically relevant IMRT plans. Effort has been concentrated on a prototype 6 MV FFF beam from an Elekta Synergy linear accelerator. This is a research unit that does not operate in clinical mode. Although the eventual aim is to demonstrate a difference in calculation accuracy between FFF and conventional beams, the aim of this work is to demonstrate the adaptability of the VSM for FFF MC dose calculations.

II. MATERIALS AND METHODS

II.A. VSM—Source densities and particle fluence distribution

For MC simulations, a beam can be described by the phase space parameters (position, direction of motion, and energy) of the constituent photons and electrons. It is possible to generate these parameters analytically in a phase space plane in front of the patient and use MC transport for particles passing through the patient. A virtual source model allows for efficient generation of particle parameters and can be commissioned for conventional linear accelerators with semiautomatic modeling tools. The VSM-based MC computes dose in the following way:

(1) Source type, energy, position, and direction of particles are sampled from the VSM. The required number of particles is generated on the fly in an arbitrary plane above the collimators to achieve a predefined level of statistical noise in the patient.
(2) The particles are transported through collimators or transmission probability filters,[12] e.g., in the multileaf collimator (MLC) plane.
(3) The dose deposited in the patient is calculated using the XVMC code.[13,14]

The VSM treats particles coming from different parts of the accelerator as if they were coming from three different virtual sources. These sources are the primary photon source, the secondary photon source, and the electron contamination source, with relative contributions P_{pri}, P_{sec}, and P_{econ}, respectively. The primary source is defined in the plane of the electron beam target where primary photons originate from interactions within the target. The secondary source models all of the photons that result from interactions occurring in places other than the target. The positions of the secondary source and the electron contamination source are free parameters which are set according to the machine geometry. The secondary source is located at the base of the primary collimator and the electron contamination source at the base of the FF (or the build-up plate).

It is assumed that each of the sources has a Gaussian shape with standard deviations σ_{pri}, $\sigma_{\mathrm{sec}}(E)$, and $\sigma_{\mathrm{econ}}(E)$ for primary photon distribution, energy-dependent secondary photon distribution, and energy-dependent electron contribution, respectively, according to the following expressions:

$$\sigma_{\mathrm{sec}}(E) = \Sigma_{\mathrm{sec}}\left(\frac{E}{E_0}\right)^{-0.34} \quad \text{if E} \geq 0.511 \text{ MeV}, \tag{1}$$

$$\sigma_{\mathrm{sec}}(E) = \Sigma_{\mathrm{sec}}\left(\frac{0.511}{E_0}\right)^{-0.34} \quad \text{if E} < 0.511 \text{ MeV}, \tag{2}$$

where E = particle energy, $E_0 = 1$ MeV, and Σ_{sec} = free parameter, the base data standard deviation of the secondary source, and

$$\sigma_{\mathrm{econ}}(E) = \Sigma_{\mathrm{econ}}(E/E_0)^{-0.18}, \tag{3}$$

where Σ_{econ} = free parameter, the base data standard deviation of the electron source.

Upon generation of a photon in the source location, the particle fluence in a phase space plane that is located above the collimators is initially flat. The particle weight is altered depending on the angle between its direction and the central axis (CAX) according to a tabulated profile. While it is possible to measure the energy fluence in air with a small detector fitted with a build-up cap, it proves more robust to measure a cross-profile in a water tank at the dose maximum (D_{max}) and determine the table by forming the ratio of the measurement to a simulation with a pristine, flat energy fluence.

II.B. VSM—Energy spectra

The primary photon spectrum (S_{pri}) on the central axis before the flattening filter is described by

$$S_{\text{pri}}(E) = \omega_0 \quad \text{if} \quad E_{\text{bin}} \le E < E_{\min}, \tag{4}$$

$$S_{\text{pri}}(E) = \left(\frac{E}{E_{\max}}\right)^{-b_{\text{pri}}} - 1 \text{ if } E \ge E_{\min}, \tag{5}$$

where E = photon energy (MeV), $E_{\min}$ and $E_{\max}$ are minimum and maximum photon energies.

For $E_{\min}$, a fixed value of 0.5 MeV is used. ω_0 = low energy bin parameter. b_{pri} = free parameter.

In the implementation of this VSM for flattened beams, this primary spectrum is attenuated with an appropriate, radially dependent filter function.[11]

The secondary photon spectrum $S_{\text{sec}}(E)$ describes the secondary photons on the CAX after the flattening filter.

$$S_{\text{sec}}(E) = \omega_S \quad \text{if } E_{\text{bin}} \le E < E_{\min}, \tag{6}$$

$$S_{\text{sec}}(E) = e^{-b_{\text{sec}}E} - e^{-b_{\text{sec}}E_{\max}} \quad \text{if } E \ge E_{\min}, \tag{7}$$

where E_{bin}, ω_S = low energy bin parameters and b_{sec} = free parameter.

The off-axis energy softening is approximated by using two parameters (δb_{pri} and δb_{sec}) which define the relative change of the primary and secondary spectra with respect to the tangent of angle to the CAX [tan(ν)] at the scoring plane

$$b_{\text{pri}}(\nu) = b_{\text{pri}} + \delta b_{\text{pri}} \tan(\nu), \tag{8}$$

$$b_{\text{sec}}(\nu) = b_{\text{sec}} + \delta b_{\text{sec}} \tan(\nu). \tag{9}$$

The energy spectrum of the contaminating electrons is approximated by an exponential function

$$S_{\text{con}}(E) = N_e \exp\left(-\frac{E}{\langle E_e \rangle}\right), \tag{10}$$

where N_e = normalization factor and $\langle E_e \rangle$ = mean electron energy.

The VSM is defined by fixed and open parameters. Fixed parameters are derived from a BEAMnrc simulation of the treatment head which is performed only for a given accelerator type. Open parameters are fitted in the polyenergetic kernel superposition commissioning routine for each individual linac.[13] The free parameters of the VSM are derived from basic beam data measurements performed in water and by minimizing the differences between calculated and measured data.

For the purpose of verifying the dose calculation accuracy of this model, the Monaco™ treatment planning system (TPS) (Elekta CMS software, St. Louis, MO) was used (version 3.1), which incorporates a commercial implementation of this model (VSM v.1.6).

II.C. FFF accelerator and beam properties

An Elekta Precise linear accelerator has been modified to enable irradiation both with and without the FF. In practice, the filter cannot simply be removed but needs to be replaced by a thin metal "enhancer" plate in the same position as the FF. This plate generates electrons which provide build-up dose to the ionization chamber to give sufficient signal to the servo plates so they, in turn, can operate properly to control the beam quality and steering.[8] Several materials and thicknesses of materials have been used in previous studies and these have recently been reviewed by Georg *et al.*[15] This prototype Elekta unit uses a 2 mm stainless steel plate which provides sufficient dose to the chamber without adding significantly to scatter. The differential attenuation of this plate can be neglected; in contrast, the overall rather large filter effect of the FF removes photons below about 1 MV almost completely on the CAX, and decreasingly toward the field edge. Dosimetric data for a linac operating with this combination of plate and energy have not been reported in the literature. These differences are briefly summarized below.

II.C.1. Depth dose slope

Without the beam hardening effect of the filter, the depth dose (DD) beyond $D_{\max}$ for unflattened beams are close to those of flattened 5 MV beams. For the machine used in this work, the beam energy has been raised back to 6 MV on the central axis by matching the quality index $\text{QI/TPR}_{20/10}$ (0.675) to the clinical 6 MV (flattened) beam.

II.C.2. Surface dose

Filter removal leads to an increase in the number of low energy x-rays (softer beam spectrum) which acts to increase the surface dose. Counterbalancing this is a reduction in electron contamination, especially at high electron energies. Measurements and MC simulations in the build-up region of unflattened beams indicate that, at 6 MV, this leads to a slight overall decrease in the surface dose. The variation with field size is also reduced for these beams compared to standard flattened beams (by approximately half).

II.C.3. Dose maximum

The softer spectrum moves $D_{\max}$ closer to the surface, whereas a lower contribution from photon scatter and electron contamination moves $D_{\max}$ deeper. Both effects almost cancel out in practice.

II.C.4. Lateral profiles

Without angular-dependent differential attenuation, there is a relatively small off-axis softening for FFF beams. Low spectral variation across the field (beam quality) results in less variation in the shape of lateral profiles with depth. Reduced head scatter (Sc) also results in lower doses outside of the field, which also falls off faster with distance. Small field sizes are relatively unaffected by filter removal, but beyond approximately 10×10 cm^2, the triangular shape of beam profiles is apparent, and photon fluence starts to decrease.

II.C.5. Head scatter

The FF is known to be the main component contributing to variation of head scatter in the treatment head. These

variations must be accurately modeled if dose calculations are to be correctly performed. The head scatter factor is seen to vary by 3% between field sizes of 3×3 and 40×40 cm^2 with the FFF machine compared to 9% for the standard 6 MV beam. The collimator exchange effect is also reduced by filter removal.[1]

II.C.6. Dose rate

The FF is composed of several centimeters of high Z materials, and one of the most immediate consequences of filter removal is the increase in dose rate. Measurements on the central axis indicate an increase in dose rate by a factor of 1.7 to 800 MU per min. Dose rates of 1200 MU per min are expected in the clinical version. If high dose rates are not required, the linac can simply run at a lower rate by changing the pulse repetition frequency (PRF). These gains in dose rate are effectively due to an increase in the dose per pulse, so regardless of PRF/dose rate, the ion recombination factors needed for accurate dosimetry should be investigated.

II.D. Model commissioning

Measurements for beam modeling included depth dose curves and profiles for various field sizes measured in a water phantom (Blue Phantom2, IBA Dosimetry, Germany). Measurements were performed at SSD = 100 cm with suitable detectors [CC01, CC13 IBA Dosimetry, NE2577 Nuclear Enterprises Ltd. (now QADOS, UK)]. Monaco is used clinically in our department with conventional flattened beams and the data set and equipment used for FFF measurements matched those originally used to commission this beam energy. In this way, the FFF and FF data can be said to be of the same standard and can be directly compared against one another.

The measurement set consisted of the following:

- Depth dose curves for field sizes: 2, 3, 5, 10, 15, 20, 30, and 40 cm^2.
- In-plane and cross-plane profiles for field sizes: 2, 3, 5, 10, 15, 20, and 30 cm^2 at depths of 1.5, 5, 10, and 20 cm.
- Diagonal profiles for the largest field size: 40×40 cm^2.
- Output factors for square fields: 2, 3, 5, 10, 20, 30, and 40 cm^2 at 10 cm depth.

The unique feature of the VSM is that it represents the primary photon spectrum before it reaches the flattening filter. Therefore, turning off the flattening filter correction corresponds to physically removing the flattening filter from the accelerator head. The procedure for modeling the FFF machine is very similar to modeling a standard machine and as a starting point a previously created model of the FF linear accelerator from the same vendor was used. The model parameters were modified as follows:

(1) The radially dependent, differential attenuation of the FF in the conventional model was turned off. Further variations in off-axis spectrum were kept constant [Eq. (8)].
(2) The relative contribution from primary photons P_{pri} was increased.
(3) $E_{\max}$ was increased along with b_{pri} to provide a better agreement of the depth dose, especially in the $D_{\max}$ region. This accounts for the retuning of the machine to produce a typical 6 MV quality index.
(4) The secondary source Gaussian sigma was made wider by a factor of $\sim$2 due to the fact that in the absence of the flattening filter, the primary collimator contributes most of the scatter.
(5) To correct the fluence profile for FFF beams, the tabulated parameters for radial energy fluence variation were adjusted to the diagonal cross-profiles at $D_{\max}$.

The results of the VSM phase space reconstruction are independent of the dose calculation engine used; therefore, it can be coupled with other MC dose engines. MC simulation and treatment planning were performed in the Monaco TPS using a water phantom of size $50 \times 50 \times 35$ cm^3. The voxel size was set at 2 mm for the smallest 2×2 cm^2 field and 3 mm for the rest of the fields with statistical uncertainties set to 0.5%.

II.E. Treatment planning

In order to expose the FFF model to a range of conditions and test the beam model and the accuracy of the dose calculation (and delivery), a series of treatments with increasing complexity and treatment volume were planned. These sites consisted of skull base, esophagus, prostate, and head and neck cases.

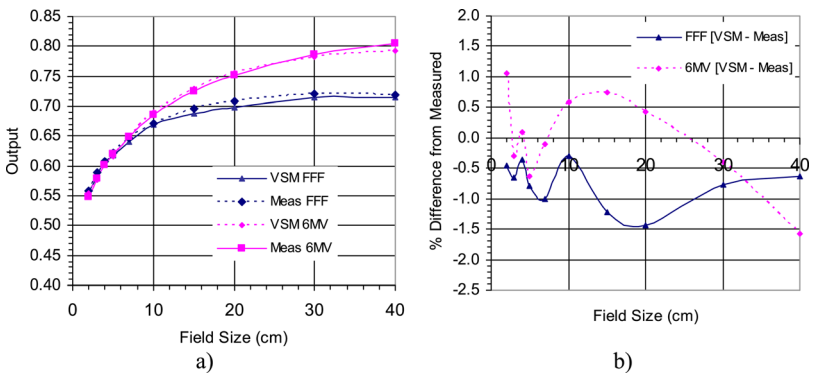

FIG. 1. (a) Absolute output factors as a function of field size for FFF and conventional 6 MV beams as predicted by the TPS compared to measurement. (b) Difference in output factors, calculated minus measured.

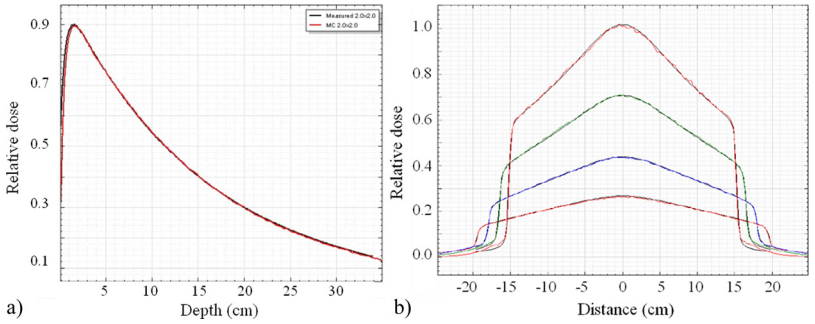

FIG. 2. Sample beam data: (a) PDD curve for 2×2 cm^2 field, (b) cross-profiles for a 30×30 cm^2 field for the FFF model.

To test the model under the extreme influence of the unflattened beams, the isocenter for the prostate and head and neck plans were placed asymmetrically so that large parts of the fields were exposed to the off-axis region of the beam.

For each plan, a set of constraints were found to give the optimal distribution. The plans were then reoptimized using the FFF beam model and adapted as necessary to fulfill the dose constraints.

These beams were then recalculated on a phantom (2%, 2 mm) for delivery to a Delta^{4PT} (ScandiDos, Inc., Sweden) IMRT verification device. All deliveries were made with the gantry at 0° to remove any influence from the treatment couch.

III. RESULTS

III.A. Water phantom data verification

Figure 1(a) shows a plot of output factor variation with field size for FFF and conventional beams, and Fig. 1(b) the difference in calculated relative output factor curve against measurement. These are absolute values as predicted by the planning system and not scaled to measured data. The absolute outputs can be predicted within 1.5% of measurements over the entire range of field sizes.

Figure 2(a) shows a sample DD curve for a 2×2 cm^2 field size and Fig. 2(b) shows profiles at depths of D_{max}, 5, 10, and 20 cm for a 30×30 cm^2 field. Figure 3 shows, for various depths and fields sizes, the percentage difference between measured and calculated depth dose curves. The spread in values is approximately 1.5% (+0.5 to −1.0) in both cases indicating that the beam model is of similar quality for both FFF [Fig. 3(a)] and conventional [Fig. 3(b)] beams, and within the measurement uncertainty for these fields. Figure 4 shows comparisons of FFF beam profile measurements against TPS predictions for field sizes from 2×2 to 30×30 cm^2 with their respective 1D γ-analysis for acceptance criteria of 2%/2 mm. It can be seen that all points had $\gamma < 0.8$. For set criteria of 1%/1 mm, 93% of all points had $\gamma < 1$.

III.B. Treatment plans

As the volume of the tumor (treatment length) and complexity of the plan increase, there is a tendency to see an underdosage in regions far from the central axis, which is seen as a sloping shoulder on the DVH curve. It is possible to compensate for this by further penalizing cold spots within the tumor, and in the Monaco TPS, this can be achieved by increasing the cell sensitivity (α) of the tumor or adding a quadratic underdose penalty. This acts to maintain plan quality but brings about an increase in both the number of segments and monitor units needed to deliver the plan. It

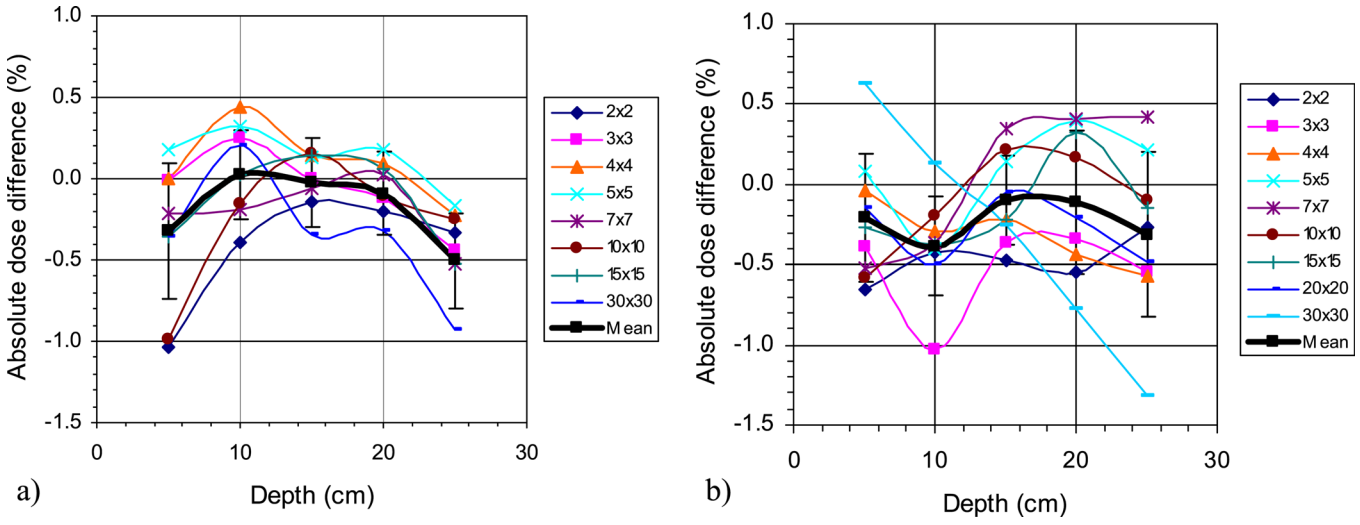

FIG. 3. Absolute dose difference between measured and calculated depth doses curves (100 cm source-surface distance) for the field sizes indicated for (a) FFF and (b) FF beams. Monte Carlo variance is set at 0.5%.

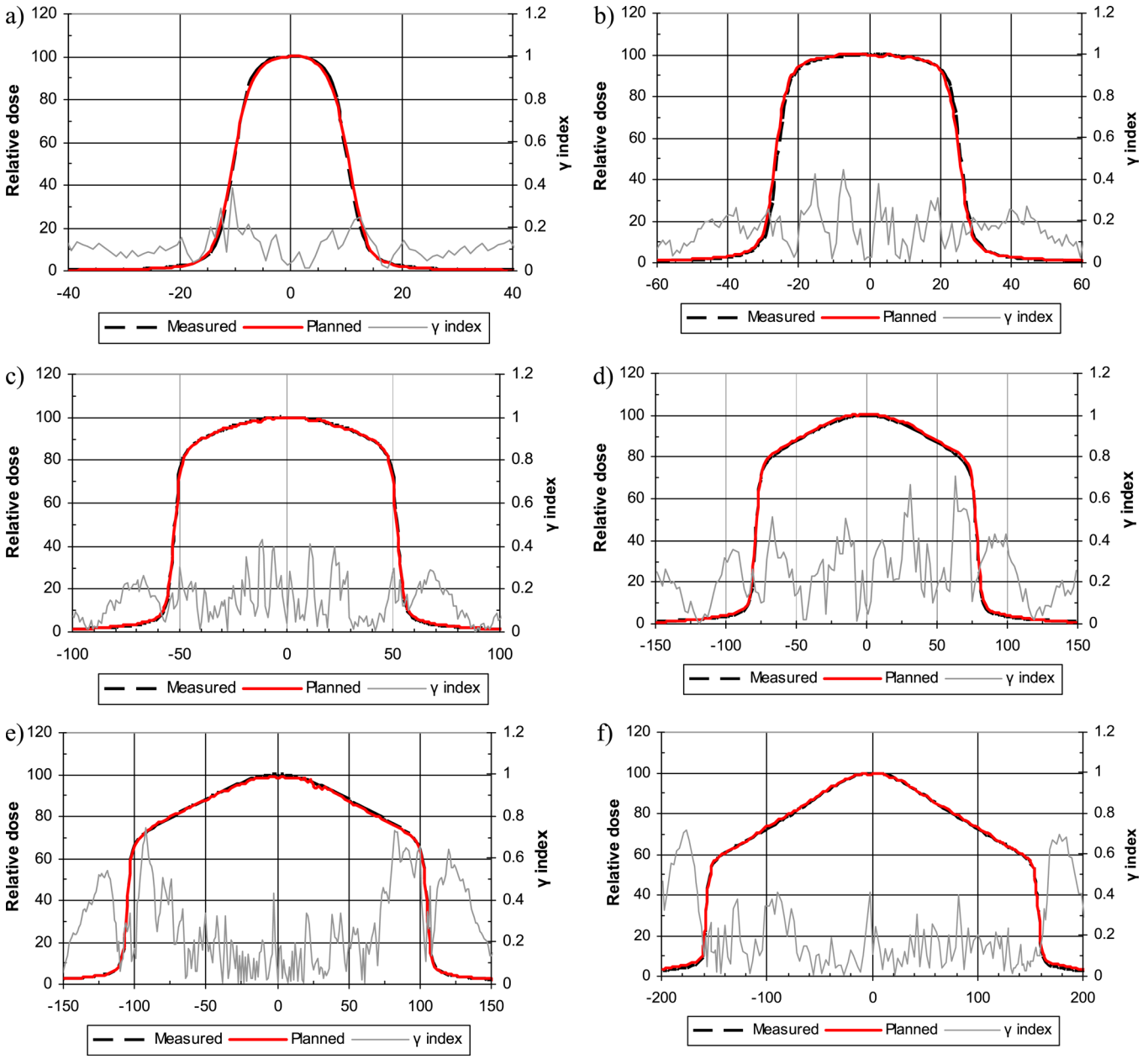

FIG. 4. Comparison of calculated vs measured beam profiles for sample field sizes of (a) 2×2 cm^2, (b) 5×5 cm^2, (c) 10×10 cm^2, (d) 15×15 cm^2, (e) 20×20 cm^2, and (f) 30×30 cm^2 at 100 cm SSD and a depth of 5 cm. Criteria for gamma analysis are 2%/2 mm.

can be seen from Table I that as the treatment volume and plan complexity increase there is a corresponding increase in the number of segments and MU needed to deliver the FFF plans. Figure 5 shows a color-wash dose distribution on sagittal and coronal CT slices through the tumor for a head and neck FFF IMRT plan. The dose volume histogram indicates that the plans are equivalent in terms of both PTV coverage and organ at risk sparing.

TABLE I. Number of segments and monitor units needed for each treatment plan and the relative increase in each necessary to deliver the FFF plans.

		Segments			Monitor units		
	PTV volume (cm^3)	6 MV	FFF	% Difference	6 MV	FFF	% Difference
Skull base	23.2	20	21	+5.0	416	446	+7.2
Esophagus	555.4	64	67	+4.7	785	931	+18.6
Prostate	804.5	66	68	+3.0	828	951	+14.9
Head and neck	918.7	168	183	+8.9	1343	1682	+25.2

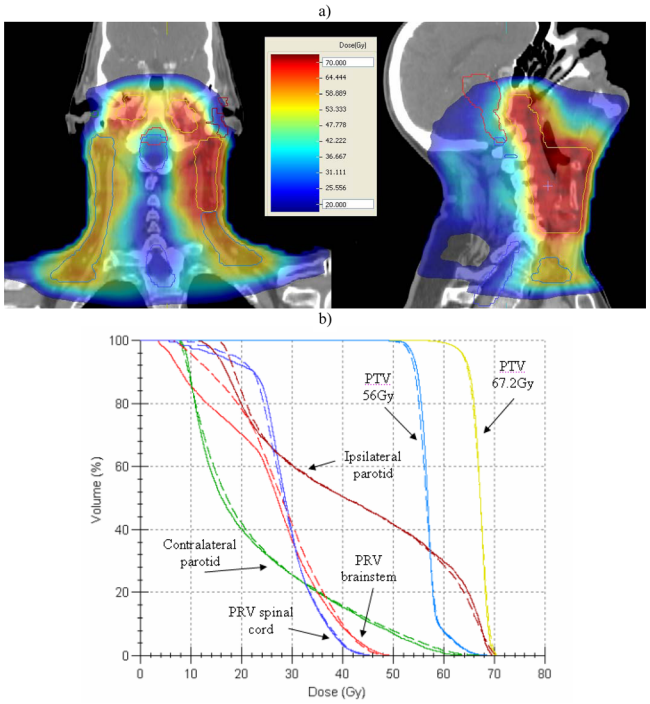

FIG. 5. Beam setup for IMRT planning of a head and neck case showing sagittal and coronal color-wash maps (a) and dose volume histogram (b). The FFF beam is displayed as the dotted line, 6 MV solid.

III.C. Verification of IMRT beams

Table II shows the absolute dose differences and statistics for the gamma analysis of the sample plans analyzed at both 3%/3 mm and 2%/2 mm acceptance criteria. It can be seen that as the volume of tumor and the complexity of the plan increase the pass rate begins to fall (as expected), but all plans pass the standard IMRT acceptance criteria of 95% of points <1 using a 3%/3 mm tolerance.

IV. DICSUSSION AND CONCLUSION

Removal of the flattening filter invalidates the assumption of energy fluence and phantom scatter homogeneity in the incident beam so a TPS must be able to model an arbitrary shape of the energy fluence. It is therefore important to be able to handle the incident particle fluence by means of a sufficiently general calculation algorithm.

The virtual source model for flattened beams was successfully adapted to a flattening filter free beam production by particle fluence warping with tabulated parameters and modifying the energy spectrum to account for the lack of angular differential absorption and general beam hardening. Since the VSM was initially derived from studies of phase spaces created by BEAMnrc,[16] it captures the salient features of the various sources of radiation in a linear accelerator without overly limiting assumptions, and thereby provides enough latitude to model flattening filter removal.

Beam modeling of the 6 MV FFF beam within Monaco is seen to be as accurate as that used clinically. Depth dose predictions are generally within 0.5% for the FFF beam, with only a few outliers up to 1% which is more consistent than for the conventional beam model. 1D gamma analysis of beam profiles for selected criteria (2%/2 mm) also show an excellent

TABLE II. Gamma analysis and absolute dose difference of individual beams for the IMRT plans. Percentage of points passing gamma analysis ($\gamma < 1$) at 3%/3 mm and 2%/2 mm for the individual beams of each plan.

		Gamma analysis 3%/3 mm		Gamma analysis 2%/2 mm		Absolute dose difference (%)	
Treatment site	Beam	6 MV	FFF	6 MV	FFF	6 MV	FFF
Skull base	1	100.0	100.0	99.5	100.0	−0.8	0.2
	2	99.8	100.0	93.5	92.4	−0.2	0.5
	3	100.0	99.8	90.6	89.4	−0.9	−0.1
	4	99.8	99.3	92.9	92.3	−0.1	0.0
	5	99.8	100.0	92.4	91.2	−0.6	0.1
Esophagus	1	100.0	99.0	98.3	89.9	0.6	1.2
	2	100.0	99.8	99.1	95.9	0.0	1.0
	3	100.0	100.0	100.0	99.8	−0.1	0.3
	4	100.0	100.0	100.0	99.1	−0.7	0.5
	5	100.0	99.8	98.8	97.2	0.2	1.0
Prostate + nodes	1	99.4	97.2	93.5	86.2	0.8	1.4
	2	99.8	100.0	97.6	98.4	0.2	0.7
	3	100.0	99.8	97.7	92.8	0.1	0.9
	4	100.0	100.0	98.8	98.8	0.0	0.7
	5	100.0	99.9	98.0	94.9	0.0	0.6
Head and neck	1	97.7	98.3	87.8	84.8	0.9	1.4
	2	100.0	98.8	97.6	94.6	0.4	1.1
	3	99.7	99.5	97.5	94.3	0.3	1.1
	4	99.5	100.0	95.7	96.9	0.3	0.9
	5	99.4	99.2	92.0	84.0	0.4	1.2
	6	99.1	98.3	94.4	87.6	0.6	1.3
	7	99.7	99.8	97.5	95.8	0.3	0.9

agreement. This matches well with commissioning results reported by Hrbacek *et al.*[17] and Kragl *et al.*[18] for FFF beams from Varian and Elekta linacs, respectively. Any differences between prediction and measurement where γ exceeded 1 occurred mainly within the out-of-field regions of the beam profiles and only for the larger ($>15 \times 15$ cm^2) field sizes.

It has been observed that as the field sizes needed for planning increase then so do the number of MU required to deliver these plans; this is a natural consequence of the FFF beam profile since it will require longer beam on times to deliver doses off-axis. The complexity of the plan is also seen to increase the number of segments required to treat the FFF plans compared to the conventional IMRT plans if plan quality is to be maintained. This may be more specifically related to the fact that segmentation algorithms used are optimized for flattened rather than unflattened beam profiles. Commercial planning systems do not currently consider the nonflat beam profile during optimization.

The optimization of nonuniform beam profiles has been discussed by Kim *et al.*[19] who reported that segment numbers required for FFF beams can be significantly reduced once this is taken into account in the optimization process. Such an addition is likely to reduce the number of segments required to deliver modulated FFF plans.

In general, the clinical implementation of this filter free design into a commercially available treatment planning system (Monaco) shows excellent results. Commissioning of the model can be performed by the same set of standard water phantom data as for the flattened beam models. These measurements need not be overly sophisticated and hence help to avoid errors in the commissioning process.

All beams for the planning exercises passed the defined acceptance criteria used for standard IMRT patient specific quality assurance tests. Once the test criteria are tightened to 2%/2 mm, slight differences can be seen between the flattened and FFF deliveries, with the conventional beams generally receiving slightly higher pass rates. There may be several reasons for this including the increased number of segments delivered and also the fact that the linac is still a prototype (nonclinical) release. Once the Elekta FFF linac is released for clinical use with fully optimized hardware and dosimetry, these tests should be repeated to assess any possible improvements in dose calculation and delivery.

ACKNOWLEDGMENTS

The author would like to thank Kevin Brown from Elekta Crawley for assistance in setting up the FFF mode and to James Satterthwaite for helpful discussion and comments concerning the paper. Many thanks also to Rick Sims for discussions around Monaco planning and beam verification. Jason Cashmore holds a research contract with Elekta UK Ltd. to study the properties of unflattened photon beams. Sergey Golubev and Jose Luis Dumont work for Elekta CMS Software. Markus Alber works as a consultant for Elekta CMS Software.

[a]Electronic mail: jason.cashmore@uhb.nhs.uk

[1]J. Cashmore, "The characterization of unflattened photon beams from 6 MV linear accelerator," Phys. Med. Biol. **53**, 1933–1946 (2008).
[2]G. Kragl *et al.*, "Dosimetric characteristics of 6 and 10 MV unflattened photon beams," Radiother. Oncol. **93**, 141–146 (2009).
[3]M. Dalaryd *et al.*, "A Monte Carlo study of a flattening filter-free linear accelerator verified with measurements," Phys. Med. Biol. **55**, 7333–7344 (2010).
[4]O. Vassiliev, U. Titt, S. F. Kry, and F. Ponisch, "Monte Carlo study of photon fields from flattening filter-free clinical accelerator," Med. Phys. **33**(4), 820–827 (2006).
[5]O. Vassiliev *et al.*, "Dosimetric properties of photon beams from a flattening filter free clinical accelerator," Phys. Med. Biol. **51**, 1907–1917 (2006).
[6]U. Titt *et al.*, "A flattening filter free photon treatment concept evaluation with Monte Carlo," Med. Phys. **33**(6), 1595–1602 (2006).
[7]W Cho *et al.*, "Multisource modeling of flattening filter free (FFF) beam and the optimization of model parameters," Med. Phys. **38**(4), 1931–1942 (2011).
[8]J. Cashmore, M. Ramtohul, and D. Ford, "Lowering whole-body radiation doses in pediatric intensity-modulated radiotherapy through the use of unflattened photon beams," Int. J. Radiat. Oncol., Biol., Phys., **80**(4), 1220–1227 (2011).
[9]G. Kragl *et al.*, "Flattening filter free beams in SBRT and IMRT: Dosimetric assessment of peripheral doses," Z. Med. Phys. **21**(2), 91–101 (2011).
[10]M. Sikora, O. Dohm, and M. Alber, "A virtual source model of an Elekta linear accelerator with integrated mini MLC for Monte Carlo based IMRT dose calculation," Phys. Med. Biol. **52**, 4459–4463 (2007).
[11]M. Sikora and M. Alber, "A virtual source model of electron contamination of a therapeutic photon beam," Phys. Med. Biol. **54**(24), 7329–7344 (2009).
[12]M. Sikora, "Virtual source modelling of photon beams for Monte Carlo based radiation therapy treatment planning," Ph.D. dissertation, University of Bergen, Norway, 2011.
[13]M. Fippel, "Fast Monte Carlo dose calculation for photon beams based on the VMC electron algorithm," Med. Phys. **26**, 867–878 (1999).
[14]J. Kawrakow and M. Fippel, "Investigation of variance reduction techniques for Monte Carlo calculation using XVMC," Phys. Med. Biol. **45**, 2163–2183 (2000).
[15]D. Georg, T. Knoos, and B. McClean, "Current status and perspective of flattening filter free photon beams," Med. Phys. **38**(3), 1280–1293 (2011).
[16]D. W. O. Rogers *et al.*, "BEAM: A Monte Carlo code to simulate radiotherapy treatment units," Med. Phys. **22**, 503–524 (1995).
[17]J. Hrbacek, S Lang, and S. Klock, "Commissioning of photon beams of a flattening filter-free linear accelerator and the accuracy of beam modeling using an anisotropic analytical algorithm," Int. J. Radiat. Oncol., Biol., Phys. **80**(4), 1228–1237 (2011).
[18]G. Kragl, D. Albrich, and D. Georg, "Radiation therapy with unflattened photon beams: Dosimetric accuracy of advanced dose calculation algorithms," Radiother. Oncol. **100**, 417–423 (2011).
[19]T. Kim *et al.*, "Inverse planning for IMRT with nonuniform beam profiles using total-variation regularization (TVR)," Med. Phys. **38**(1), 57–66 (2010).